Effect of Acoustic Environment on the Burning Rate of Solid Propellants

J. E. Crump* and E. W. Price†
U. S Naval Ordnance Test Station, China Lake, Calif.

During unstable combustion of solid propellants, the burning surface is exposed to severe oscillations in the adjoining gas environment, and large changes in burning rate of the propellant result. By using specially designed burners, it was found possible to determine, by interrupting burning, the effect on the propellant burning rate. Because of the standing-wave nature of the oscillatory behavior, it was possible to correlate the change in burning rate at each point on the propellant surface with the nature of the acoustic environment. It was observed that burning rate is decreased by acoustic pressure and increased by acoustic velocity (double-base propellants), the two effects being of comparable magnitude. The fluctuations in equilibrium pressure during unstable rocket motor and vented vessel firings were found to be readily explainable in terms of the burning-rate effects obtained from the interrupted burning tests, provided the acoustic behavior during the firings was simple enough to analyze. However, a singular class of behavior was observed under certain conditions; dramatic increases in burning rate occurred at characteristic times during burning when the frequency of the unstable tangential mode (first mode) was an integral multiple of the frequency of an unstable axial mode.

Introduction

THE work reported here is concerned with determination of the changes in burning rate (surface regression rate) of solid propellants in the presence of acoustic environments encountered in rocket motors. The nature of the acoustic environments is described approximately by solutions of the wave equation as described by Morse,[1] Smith and Sprenger,[2] and McClure, Hart, and Bird.[3] In the present work, methods were developed to control the acoustic environment to a degree not previously attained in combustion experiments.

Acoustic Environments

For the standing-wave acoustic modes occurring in the systems used here, the acoustic environment due to any particular mode can be characterized by the amplitudes of the pressure oscillations and the oscillations in gas velocity parallel to the burning surface. The mode structures of the first three axial modes are illustrated in Fig. 1a, which shows the amplitude of pressure and velocity oscillations as a function of position along the length of the charge for standing axial modes. From the figure it is evident that, for any particular mode, there are locations where the amplitude of the pressure oscillations is a maximum and amplitude of the velocity oscillations is zero (pressure antinodes, velocity nodes); at other locations there is no pressure oscillation, but the amplitude of velocity oscillations is a maximum (pressure nodes, velocity antinodes). The amplitudes of the pressure and velocity oscillations at their respective antinodes are referred to here as Δp and Δu, and, for any given mode, these quantities are related[4]:

$$\Delta p/p = \gamma\ (\Delta u/a) \qquad (1)$$

where p is the mean pressure, γ is the ratio of specific heats of the gas, and a is the local velocity of sound. Most of the burning-rate data in the present paper refer to rates at pressure and velocity antinodes where the acoustic environment is relatively simple.

In the series of tests on catastrophic burning-rate changes, the acoustic environment was complicated by the concurrent presence of oscillations in both axial and transverse modes. Indeed, the phenomenon was critically dependent on the presence of both types of oscillations. The nature of these modes has been detailed in Refs. 1–3, and the structure of the first tangential mode is indicated in Fig. 1. It is important for the later discussion to note that the frequency of any transverse mode decreases during burning due to the increasing diameter of the perforation of the propellant sample. On the other hand, the frequency of each axial mode is substantially constant during burning.

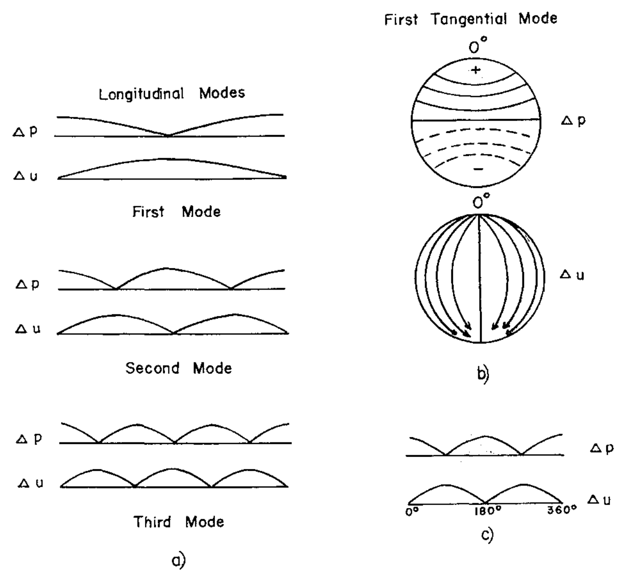

Fig. 1 Representation of the space-distributed nature of two types of acoustic modes of circular cylindrical closed cavities: a) the first three longitudinal modes; b) the first stationary tangential mode, general distribution; and c) the first tangential mode as a function of position along circumference of boundary.

Presented as Preprint 64-141 at the Acoustic Combustion Instability session (cosponsored by the Department of Defense Technical Panel on Solid Propellant Instability of Combustion) at the AIAA Solid Propellant Rocket Conference, Palo Alto, Calif., January 29–31, 1964; revision received March 13, 1964.

* Physicist, Aerothermochemistry Group. Member AIAA.
† Head, Aerothermochemistry Group. Associate Fellow Member AIAA.

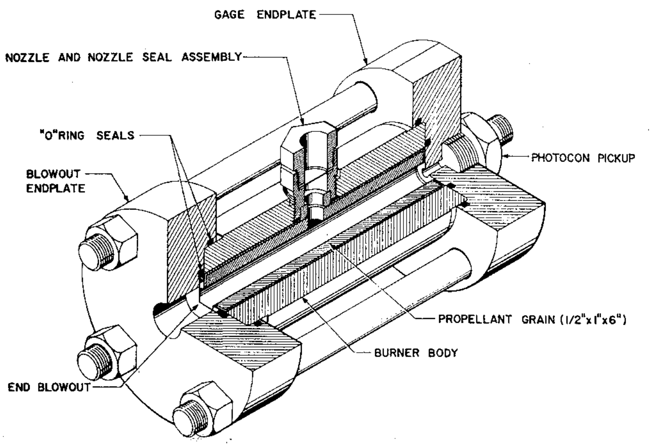

Fig. 2 The Naval Ordnance Test Station combustion instability tubular burner. Tubular propellant charge is 1.0-in. o.d.

Experimental Methods

Burning-rate measurements have been made in two types of systems. One system,[5] a T-burner used by Eisel, has been useful in determining the burning-rate changes due to acoustic pressure as a function of frequency and mean pressure.

The other system, from which the burning-rate data in the present report were obtained, is shown in Fig. 2.[6–10] The acoustic environment is generated by spontaneously unstable combustion, and the burning-rate is determined by interruption of burning and measurement of the partially burned charge. In one series of tests, this burner produced fairly constant amplitude oscillations, primarily in the first axial mode. In some of the tests, resonant cavity dampers were installed in the endplates and tuned to the other acoustic modes in order to suppress unwanted modes.

In all experiments, pressure measurements were made with high-frequency response systems, whose characteristics are detailed in Refs. 6 and 7. Interruption of burning was usually accomplished by sudden pressure reduction resulting from mechanical release of a diaphragm. A water-quench system was used in some tests where depressurization alone was not effective in interrupting burning.

Burning-Rate Changes in Simple Acoustic Environments

The majority of the tests in which quantitative determinations of burning rate were made were conducted in the type of burner shown in Fig. 2, with the oscillatory behavior occurring predominantly in the first longitudinal mode at 4200 cps at fairly constant amplitude. The actual harmonic content of a typical test in which no resonator was used is illustrated by the amplitude-frequency analysis in Fig. 3.

Normal test procedure consisted of loading a previously measured propellant charge into the burner, initiation of burning with a hot wire and loose powder train in the burner, and interruption of burning by mechanical release of the shear disk in the end of the burner. The severity of the oscillatory behavior was estimated from the amplitude of the pressure oscillations in an oscilloscope record. The partially burned charge was measured at several points along its length. The average burning rate r at each point was calculated from the distance burned and the burning time. This burning rate was compared with the burning rate r_0 to be expected under stable conditions at the pressure of the test. A change in burning rate was determined as the difference between observed and normal burning rate and was normalized by taking the ratio

$$(r - r_0)/r_0 = (r/r_0) - 1$$

This calculation was made for the several points along the charge, and the resulting data were plotted as percentage change in burning rate as a function of position along the charge.

In the foregoing procedure, there is some difficulty in determining an appropriate value for the "normal" burning rate r_0, primarily because strand burning-rate data for the same propellants do not duplicate the radial burning of the tubular samples. There is also some error involved in the effects of nonsteady burning at the start and end of the tests and in the averaging of burning rate over the more slowly changing mean pressure during the balance of the test. Because of these uncertainties in determining r_0, the experiment was modified by the addition of a stable second burner that burned a control sample of propellant (Fig. 4). The two burners were connected by a manifold, and both burners discharged through the same nozzle. Burning was initiated and interrupted in both burners simultaneously, so that both propellant samples experienced the same steady-state pressure-time history during burning (Fig. 5). The two burners were acoustically decoupled by appropriate location of the manifold, use of burners of different length and mode frequencies, and use of an acoustic filter in the manifold. The burner with the control sample was stabilized by use of a half-length charge situated midway between the ends of the burner cavity (this places the combustion in an unfavorable location for driving oscillations[6]) and by use of a loose-fitting propellant sample that provides attenuation of oscillations.[6, 7]

These methods resulted in reduction of oscillations in the control burner to amplitudes of about 1% of those in the test burner (Fig. 5). The control samples showed uniform web thickness after the test. Because the test sample and control sample experience the same pressure-time history, the burning-rate changes are obtained by taking the ratio of the change in

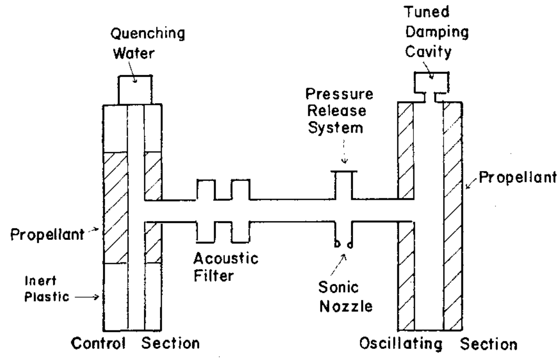

Fig. 4 Internal arrangement of double burner.

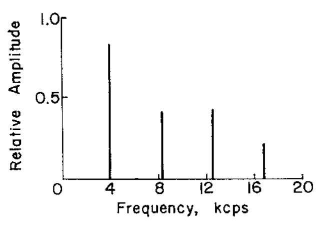

Fig. 3 Harmonic analysis of pressure oscillations showing relative strength of the longitudinal modes for a JPN propellant test in the burner in Fig. 2.

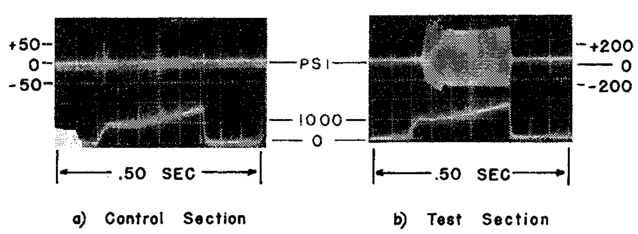

Fig. 5 Pressure-time records for a typical test in the double burner described in Fig. 4, showing mean and oscillatory pressures in both sections of burner.

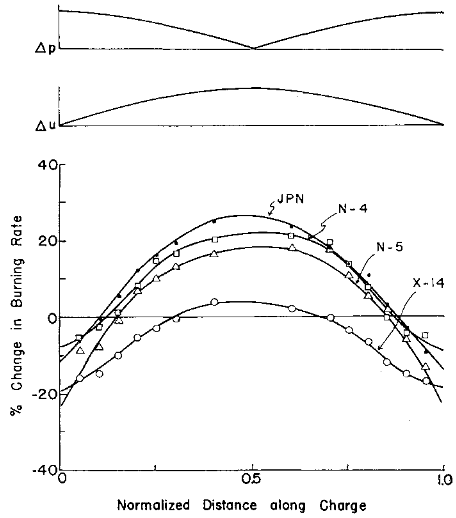

Fig. 6 Change in burning rate as a function of acoustic environment for combustion oscillations at 4200 cps for four double-base propellants. The mean steady pressure was 1100 psi for JPN, 1300 psi for N-4, 1300 psi for N-5, and 1400 psi for X-14.

web thickness of the test sample to the change in web thickness in the control sample.

Results in Simple Environments

Tests in the double burner were run with several propellants, the majority being with extruded double-base formulations. Representative data for four double-base propellants are shown in Fig. 6; typical data for an ammonium perchlorate-PBAA propellant are shown in Fig. 7. From more than 20 tests with both double-base and composite propellants, it was observed that the burning rate was always abnormally high in the middle part of the charge where the acoustic environment consisted predominantly of gas oscillations parallel to the burning surface (see first mode structure in Figs. 1, 6, and 7). For all of the double-base propellants, a depression in burning rate at the pressure antinode was observed. Also, for the double-base propellants, the magnitudes of the changes in burning rate at the pressure and velocity antinodes were seen to be roughly equal, a point that dramatizes the view that the effect on the equilibrium pressure in the rocket motor will be dependent on the interplay of these two opposing effects integrated over the whole charge surface.

In the case of JPN propellant, tests were run with different severity of oscillatory combustion, so that the change in burning rate could be determined as a function of severity. The severity of oscillations was determined from the pressure records, and the amplitude of the velocity oscillations was then calculated from Eq. (1). The changes in burning rate could then be referred to the amplitude of either pressure or velocity oscillations. The percentage change in burning rate at the velocity antinode‡ is shown as a function of ($\gamma\ \Delta u/a$) in Fig. 8, where it is seen that the burning rate increases linearly with severity of oscillations, with some indication of a threshold severity for onset of burning-rate increases. For the larger amplitudes, the determination of Δu is probably rather inaccurate, but the scale is still an aid to physical insight.

Figure 8 also shows the changes in burning rate at the pressure antinode determined for JPN propellant. Although the data scatter badly, it seems evident that the decrease in burning rate becomes rather insensitive to severity of oscillations after $\Delta p/p$ reaches about 0.4.

Several "standard" composite propellants were burned in attempts to obtain "irregular burning-rate" data; however, all of the standard types either could not be effectively partially burned or, after a partial burn, the surface was too rough to yield meaningful measurements. The composite propellant data reported here were obtained from a specially formulated composition using 70% ammonium perchlorate (Mikropulverized), 1.75% copper chromite, and PBAA. This combination yielded a propellant that could be mixed, cast, and cured with very little bubble formation, that could be partially burned (using rapid depressurization and water-quenching techniques), and that, because of lack of bubbles and the small AP particle size, had a relatively smooth partially burned surface.

Although the accuracy of web-thickness measurements was very poor with the composite propellant because of surface

‡ Burning rates at the velocity antinode were determined from interpolation to the 0.5 point on curves like those in Fig. 6 rather than by actual measurements at the antinode. Because of the vent hole in the charge wall at the midpoint (velocity antinode), distortion of the flow field produced local anomalies in burning rate there. Similarly, the burning rates at the pressure antinodes were determined by extrapolation of the measured data to the 0 and 1 positions on the normalized length scales, since local anomalies in rate occurred at these locations because of the use of inhibiting materials on the ends of the charges.

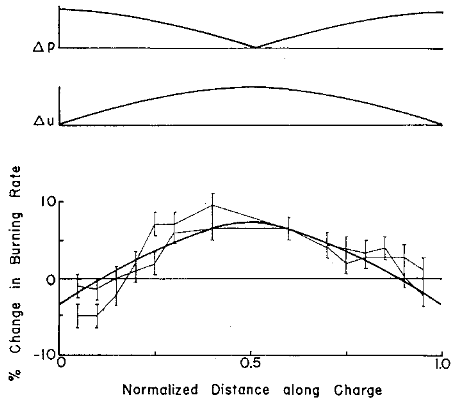

Fig. 7 Change in burning rate as a function of acoustic environment for combustion oscillations at 4200 cps for AP-PBAA composite propellant. Broken lines indicate web-thickness measurements along two mutually perpendicular axial planes; smooth curve is best estimate of burning-rate changes. The mean steady pressure was 300 psi.

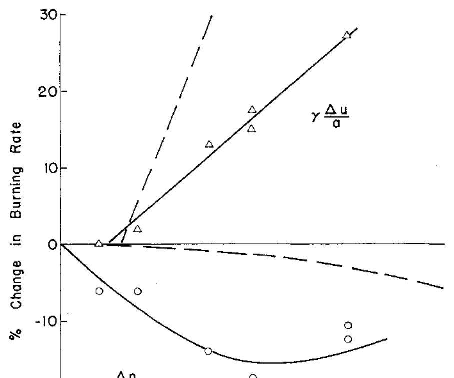

Fig. 8 Change in burning rate at the pressure and velocity antinodes for JPN propellant at 4200 cps. Solid lines are the correlation of experimental oscillatory data; dashed lines indicate changes that would be expected if burning rate had conformed to normal steady-state behavior.

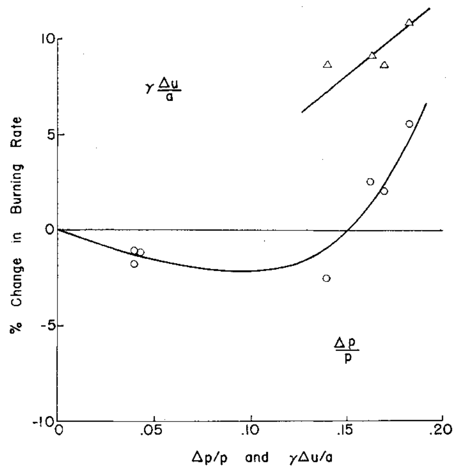

Fig. 9 Change in burning rate at the pressure and velocity antinodes for the AP-PBAA composite propellant.

roughness (as indicated in Fig. 7), enough data were obtained to determine crudely the change in burning rate as a function of severity for the composite propellant as was done for JPN propellant. These data are shown in Fig. 9. As was the case for JPN, it is seen that the increase in burning rate at the velocity antinode varies linearly with severity of oscillations. Figure 9 also shows the changes in burning rate at the pressure antinode. The three data points near $\Delta p/p = 0.04$ were obtained from the "one-dimensional" system mentioned earlier (also Ref. 5). The balance were obtained from the double-burner arrangement (Fig. 4).

The data for the burning-rate change of the composite propellant at the pressure antinode are not necessarily typical of the response of all composite propellants, although, at small values of $\Delta p/p$, the trend and magnitude of the burning-rate decrease are comparable to those reported by Eisel[5] for T-35 (composite) propellant.

It may be noted that the effects of acoustic environments on burning rate for JPN propellant indicated in Fig. 6 are in the same direction as would be predicted if the burning rate conformed to the pressure and velocity dependence established under steady-state conditions. Using the erosive burning-rate data of Wimpress[11] and assuming sinusoidal oscillations of pressure and velocity [related by Eq. (1)], curves are presented in Fig. 8 indicating how the mean burning rate would vary if steady-state burning were approximated at all times. Comparison of the solid and the broken curves in the figure indicates that the effect of acoustic pressure is dramatically different from that which would be predicted by steady-state burning behavior. The contrast between "acoustic erosivity" and steady-state erosive burning is not so conspicuous, but the steady state is clearly a very poor approximation.

Referring to points on the burning surface which are not at antinodal points of the acoustic field, the burning surface is exposed to a more complicated acoustic environment consisting of both pressure and velocity oscillations. The severity of the pressure and velocity oscillations at each point can be estimated from the longitudinal acoustic mode structure as typified by Fig. 1. Assuming that the acoustic pressure and acoustic velocity effects on burning rate are additive, the data in Fig. 8 may be used to estimate combined effects on burning rate. Although the accuracy of the available data did not motivate extensive calculations of this kind, comparison of preliminary calculations with actual burning rate effects such as those in Fig. 6 indicated that the velocity and pressure effects are not additive. Instead, the interaction seemed to favor the acoustic velocity effect. Thus the burning rate of the JPN charge illustrated in Fig. 6 is above normal over most of its length. This observation is consistent with the observation that the pressure increases

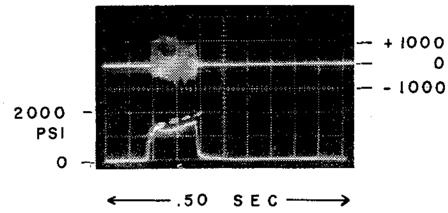

Fig. 10 Pressure-time record showing pressure decrease with mesa propellant due to effect of oscillatory combustion on the burning rate. Dashed line indicates approximate pressure-time relation without oscillatory burning.

during oscillatory combustion in vented-vessel firings of JPN propellant. As suggested by the burning-rate data on X-14 mesa propellant in Fig. 6, the pressure decreases during oscillatory combustion of that propellant in vented-vessel firings (Fig. 10).

"Catastrophic" Changes in Burning Rate

During studies of the behavior of the simple burner in Fig. 2, efforts were made to damp selectively the lower-frequency longitudinal modes. One technique was to introduce small Helmholtz resonator cavities in the blowout endplate of the burner, tuned to a low-frequency axial mode. This selective damping led to complete or partial suppression of the mode in question and, in addition, usually led to oscillatory behavior in higher axial modes at frequencies up to 22,000 cps and in tangential modes from 24,000 to 48,000 cps.

The most conspicuous feature of these tests, however, was the occurrence of violent pressure spikes, the rates of pressure rise being on the order of 100,000 psi/sec (Fig. 11). The magnitude of the pressure spikes suggested much higher perturbations in surface-average burning rate than were consistent with the behavior described in the last section. Initial studies of this phenomenon[12] showed that the pressure spikes occurred at characteristic times during burning and that high-frequency oscillations were conspicuous preceding and during the pressure rise. Although the frequency response of the pressure-detection system rendered quantitative measurement of the amplitude of the high-frequency oscillations impractical, the oscillations were easily recorded.

Results in Complex Environments

Careful examination of high-speed pressure records revealed that, when these "catastrophic" pressure peaks occurred, oscillations in both axial and tangential modes were present. Furthermore, it was observed that the peaks occurred at times when the frequency of the tangential mode was an integral multiple of the frequency of an unstable axial mode. This relation was verified for a large number of catastrophic peaks, in some cases with more than one peak in the same firing.

An effort was made to determine whether a "castastrophic" peak was caused by an increase in amplitude of the harmonically related modes or only by the occurrence of the harmonic relation. Special narrow-band-pass filters that allowed resolution and recording of each axial mode on a different recording channel were used during some of the tests. How-

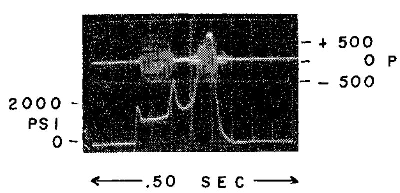

Fig. 11 Pressure-time record showing "catastrophic" pressure peaks using the burner shown in Fig. 2.

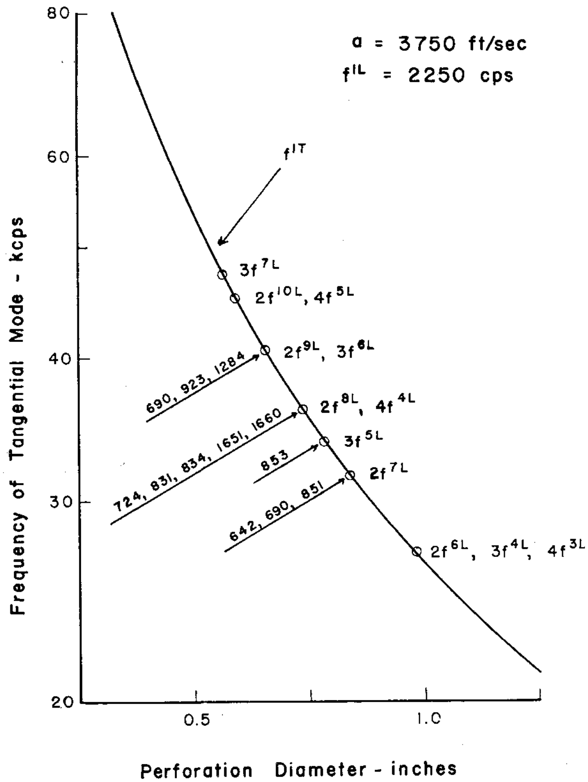

Fig. 12 Some harmonic relationships that occur between axial and tangential acoustic modes during burning of a 0.5-in. i.d. × 1.0-in. o.d. × 10.0-in. length internal burning propellant charge. Numbers indicate tests in which the harmonic relationship noted was identified with a "catastrophic" response.

ever, because of a low signal-to-noise ratio in the instrumentation array for these tests (nos. 1284, 1651, and 1660), the objective of detecting changes in amplitude of the "guilty" modes was not accomplished.

A summary of the frequency conditions under which the majority of catastrophic peaks have been observed in the tubular burner is shown in Fig. 12. The curve represents the frequency of the first tangential mode as a function of diameter of the perforation of the propellant charge during burning. The circles mark the diameters at which a harmonic relation exists between the tangential mode and one of the higher axial modes. The labels on the circles denote the number of the axial mode and the ratio of frequencies ($3f^{5L}$ means that, at that diameter, the frequency of the first tangential mode is three times the frequency of the fifth longitudinal mode). The numbers to the left of the curve list the test numbers on which catastrophic peaks occurred, and the frequency relations that pertain are denoted by the arrows. Test no. 923 was performed with X-14 propellant; the balance of the tests were with JPN propellant.

The extent to which this "catastrophic" behavior is related to rocket-motor behavior has not been determined, although such responses have also been observed in a 1- × 6-in. nozzle-on-the-end modification of the burner. There is no obvious reason why conventional rocket designs should not exhibit the same behavior, although the "catastrophic" response might be localized in a more complex geometry, and, as a result, the pressure-time response might not be as dramatic.

References

1 Morse, P. M., *Vibration and Sound* (McGraw-Hill Book Co., Inc., New York, 1948), 2nd ed., Chap. VIII.

2 Smith, R. P. and Sprenger, D. F., "Combustion instability in solid-propellant rockets," *Fourth Symposium (International) on Combustion* (Williams and Wilkins Co., Baltimore, Md., 1953), pp. 900–903.

3 McClure, F. T., Hart, R. W., and Bird, J. F., "Acoustic resonance in solid propellant rockets," J. Appl. Phys. **31**, 884–896 (1960).

4 Liepmann, H. W. and Roshko, A., *Elements of Gasdynamics* (John Wiley and Sons, Inc., New York, 1957), p. 71.

5 Eisel, J. L., "The effect of acoustic pressure on the burning rate of solid rocket propellants," Combustion Institute, Western States Section, Sacramento, Calif., Preprint WSS/CI, Paper 62-23 (November 26–27, 1962); also Pyrodynamics **1**, 61–70 (1964).

6 Price, E. W., Mathes, H. B., Crump, J. E., and McGie, M. R., "Experimental research in combustion instability of solid propellants," Combust. Flame **5**, 149–162 (June 1961).

7 Mathes, H. B., "Measurement problems in research on unstable combustion of solid rocket propellants," *Eighth Symposium (International) on Combustion* (Williams and Wilkins Co., Baltimore, Md., 1962), pp. 894–903.

8 Price, E. W., "Experimental measurements in solid propellant rocket combustion instability," *Experimental Methods in Combustion Research* (Pergamon Press, Oxford, 1964), pp. 58–60.

9 Price, E. W., "Contribution to the round table on acoustic instability," *Eighth Symposium (International) on Combustion* (Williams and Wilkins Co., Baltimore, Md., 1962), pp. 925–929.

10 Crump, J. E. and Price, E. W., "Effect of acoustic environment on the burning rate of double-base solid propellants," ARS J. **31**, 1026–1029 (1961).

11 Wimpress, R. N., *Internal Ballistics of Solid Fuel Rockets* (McGraw-Hill Book Co., Inc., New York, 1950), p. 24.

12 Crump, J. E. and Price, E. W., " 'Catastrophic' changes in burning rate of solid propellants during combustion instability," ARS J. **30**, 705–707 (1960).